Journal Name

ARTICLE TYPE

Cite this: DOI: 10.1039/xxxxxxxxxx

A 3D antiferromagnetic ground state in a quasi-1D π-stacked charge-transfer system

Adam Berlie,*[a,b] Ian Terry,[b] and Marek Szablewski[b]

Received Date
Accepted Date

DOI: 10.1039/xxxxxxxxxx

www.rsc.org/journalname

With the rising interest in organic based materials it is important to fully understand their properties in order to identify correlations between both structural and physical properties. One material that still holds some ambiguity is triethylammonium bis-7,7,8,8-tetracyanoquinodimethane (TEA(TCNQ)$_2$).This charge transfer compound has one electron delocalised across two TCNQ molecules along quasi-1D stacks. Previous work has shown that there is magneto-electrical coupling associated with the magnetic transition, however the magnetism and ground-state is not well understood. Within this manuscript we provide evidence for a long range magnetic order that is 3D in nature.

1 Introduction

Purely organic systems have some significant advantages over inorganic or ceramic counterparts, such as relative cost of synthesis and the ease at which molecules can be changed or functionalised to enable one to "tune" their physical properties. In many cases, organic molecules can stabilise radical through delocalisation of the intrinsic electron where this leads to a playground of magnetism and distribution of electric charge. The latter can result in electronic polarisation which is one of the vital properties one looks for when searching for new ferroelectrics; it should also be noted that a combination of both magnetism and electronic charge can also lead to magneto-electric coupling, that is most commonly associated with multiferroics.

The purely organic charge-transfer molecular system TEA(TCNQ)$_2$ (triethylammonium bis-7,7,8,8-tetracyanoquinodimethane) is comprised of quasi-1D stacks of TCNQ molecules interleaved by triethylammonium cations. The compound is able to stabilise a radical electron by delocalising this across two TCNQ molecules, thus creating dimers of $S = 1/2$ magnetic entities. However, rather then having a *...ABAB...* type structure of alternating TCNQ molecules like the more famous charge transfer system MEM(TCNQ)$_2$, TEA(TCNQ)$_2$ has an *...BAA′B′...* chain like structure where the TCNQ molecules are grouped into tetramers, with an inversion centre between the A and A' molecules. An electron is therefore delocalised across the two AB molecules and one can see that there will be strong interactions not only along these quasi-1D stacks, but also within the tetramers themselves. As the temperature decreases, the distance between these TCNQ molecules also decreases leading to some intriguing physical effects.

Recent work by us has shown that there are anomalies within the temperature dependence of the capacitance and loss from performing dielectric measurements. The high temperature change in the dielectric data is consistent with the temperature where the TEA cations are believed to freeze and no longer able to flip between different orientations. This transition is accompanied by a drop in the capacitance and subsequent polarisation. A study is underway to fully understand this transition and the frequency spectrum associated with this order-disorder transition. The second, lower temperature, anomaly shows a peak in the loss data suggestive that there is a process freezing out and this is congruent with the onset of the magnetic transition in TEA(TCNQ)$_2$, that shows the characteristic behaviour of the magnetic susceptibility of a spin-Peierls (SP) system, however it is not now considered as an SP material. The dielectric data also show that there is a strong frequency dependence associated with the electronic moments associated with this magnetic transition, where it follows a similar scaling behaviour to that of a spin glass suggesting that the electronic polarisation across the TCNQ dimers may freeze at this magnetic transition in a glassy manner. It is clear however, that in order to fully understand this behaviour and the intrinsic magneto-electric coupling one must also understand the mag-

[a] *ISIS Neutron and Muon Source, Rutherford Appleton Laboratory, Science and Technology Facilities Council, Didcot, OX11 0QX, United Kingdom. E-mail: adam.berlie@stfc.ac.uk*

[b] *Department of Physics, Durham University, South Road, Durham, DH13LE, United Kingdom.*

† Electronic Supplementary Information (ESI) available: [details of any supplementary information available should be included here]. See DOI: 10.1039/b000000x/

netism within this system. Our current work presents a closer look at the ambiguous magnetic behaviour of TEA(TCNQ)$_2$ where we utilise the muon spin spectroscopy technique to better understand the nature of the transition and show that this in fact behaves more like a 3D bulk ordered system as opposed to a low dimensional system such as SP compound.

2 Experimental Methods

TEA(TCNQ)$_2$ was synthesised using the method outlined by Acker *et al.*. This produced black crystals that were used in both magnetic susceptibility and muon spectroscopy measurements. The magnetic susceptibility measurements were conducted using an Quantum Design MPMS with a 7 T superconducting solenoid magnet. The muon spin spectroscopy (known as muon spin relaxation or rotation or simply μSR) experiments were conducted on the CHRONUS spectrometer at the RIKEN-RAL muon facility in single pulse mode. A 100% spin polarised anti-muon (μ^+) ensemble, with a half life of 2.2 μs, are implanted into the sample that is placed in the centre of the spectrometer between two detector banks, one upstream (forward) and one downstream (backward). One is able to detect the evolution of the muon ensemble polarisation through the measurement of the positron emitted preferentially along the direction of the muon spin at the time of decay ($\mu^+ \rightarrow e^+ \bar{\nu}_\mu \nu_e$). The relaxation of the muon polarisation is detected through the difference or asymmetry between the forward and backward detector banks. The muon is sensitive to both static and dynamic nuclear and electronic moments where the relationship of the muon rotational frequency to the magnetic field that the muon experiences is $\omega = \gamma_\mu \mathbf{B}$, where γ_μ is the muon gyromagnetic ratio. If dynamics are present, this causes a broadening of the muon rotational frequency and one can see an exponential type relaxation. Because the muon couples through a dipolar interaction, it is purely a local probe and samples a range of approximately 2 nm. Generally there are three different types of magnetic environments one can perform experiments in; zero-field (ZF), where compensation coils are used to screen out the Earth's magnetic field, longitudinal field (LF), where a field is applied along the initial muon polarisation to decouple the muon from it's internal magnetic environment and transverse field (TF), where a magnetic field is applied perpendicular to the initial muon polarisation that causes the muon spin to precess in the vector sum of applied and internal fields.

3 Results and Discussion

The magnetic susceptibility of the sample is shown in Figure 1 and has a distinctive shape similar to that of a spin-Peierls system, however at low temperature, paramagnetism dominates which is likely due to defects rather then chemical impurities. In order to quantify the data, a diamagnetic background of -2.22×10^{-8} m^{3}kg^{-1} was subtracted. The data were then fit using the formula:

$$\chi = D \cdot \exp(-E_a/T) + C/(T-\theta) \quad (1)$$

Where the first term represents the opening of a spin gap where D is the pre-exponent and E_a is the activation energy and the second term is the Curie-Weiss law, that accounts for the defects states within the crystal. The parameters from the fit can be seen in Table 1. Previous analysis of dielectric data through the transition gave an activation energy of 423 K (CITE!!!) and this is similar to that obtained from the magnetic measurement. This behaviour is indicative of the opening of a spin gap where the TCNQ dimers enter a singlet phase. The low temperature upturn is likely due to defect states; using the Curie Constant, C, to extract a number density, N, keeping $g = 2$ and $J = 1/2$, $N = 1.1 \times 10^{22}$ kg^{-1} and this accounts for approximately 1% of the sample. Therefore this can be considered a minor phase. The non-zero value of θ may indicate that there is some magnetic exchange associated with the defect states, something that has been observed in another TCNQ based spin-Peierls compound(CITE). Since the magnetic susceptibility measurements were collected in 5 T, this can act to broaden out the transitions as well as cause the signal from the low temperature defect state to increase thus polluting the data despite being a minor component. Therefore to further understand the magnetic transition a more local probe is needed such as μSR.

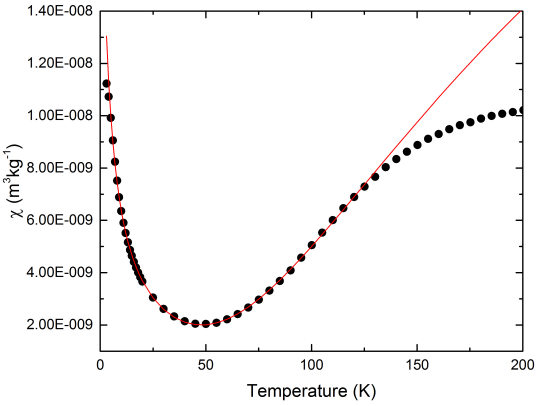

Fig. 1 Magnetic Susceptibility of TEA(TCNQ)$_2$ taken in an applied field of 5 T. The solid line is a fit to the data as described in the main text.

Table 1 Parameters from fit to the magnetic susceptibility

Parameter	Value
D	$4.4(1) \times 10^{-8}$ m^{3}kg^{-1}
E_a	237(3) K
C	$8.7(1) \times 10^{-8}$ m^{3}kg^{-1}K^{-1}
θ	-3.7(2) K

Since μSR is a local probe, this means that the defect states are significantly dilute that they will not impact the data. Additionally, since μSR is also sensitive to dynamics on the MHz time scale, any paramagnetic states are motionally narrowed at the high temperatures where the magnetic transition is present. μSR data were collected in both zero field (ZF) and in an applied transverse field (TF) of 50 G.

The ZF raw data were best fit from from 10 to 200 K using the equation:

$$G(t) = A_{ZF} \exp(-\sigma^2 t^2) \cdot \exp(-\lambda_{ZF} t) + A_B, \quad (2)$$

where A_{ZF} is the relaxing asymmetry, σ is the relaxation due

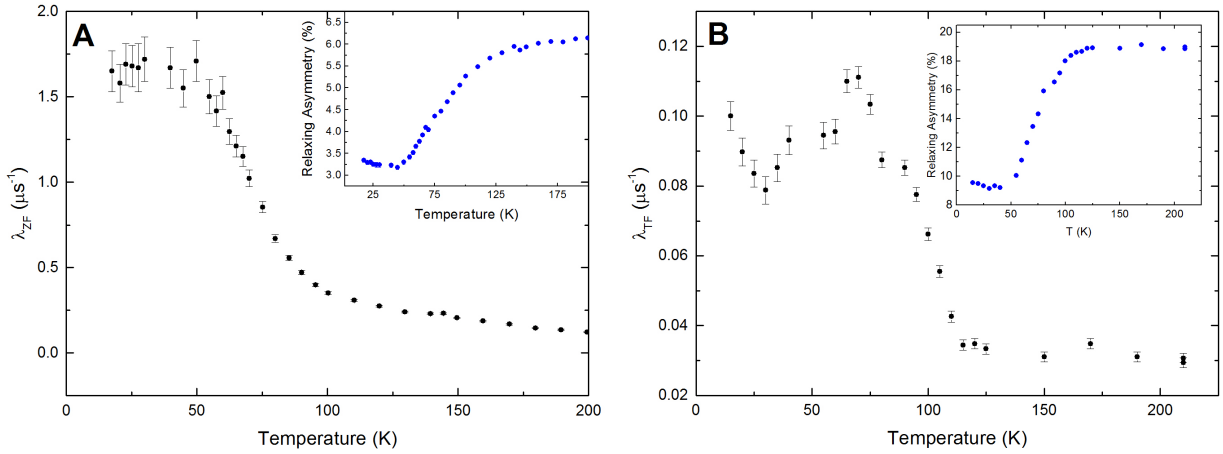

Fig. 2 A: The zero-field muon spin relaxation as a function of temperature. **B:** The muon spin relaxation in an applied transverse field of 50 G as a function of temperature. Both insets show the respective relaxing asymmetries.

to coupling of the muon to a nuclear component that was fixed at 0.26 μs^{-1}, λ_{ZF} is the muon relaxation and A_B is the baseline accounting for non-relaxing muons stopping in the cryostat and sample plate that was fixed at 2.5%. In this case, it λ_{ZF} is that is modelling the dynamics of the electronic moments where $\lambda \propto 1/\nu$, the fluctuation rate of the electronic moments. σ accounts for a static field distribution that is a result of the multitude of nuclear moments in the sample where the multiplication of the two terms represents a modulation of this field distribution by the onset of electronic fluctuations. At the high temperatures the muon relaxation is flat however on approaching the transition, the fluctuation rate of the electronic moments enters the time scale of the measurement and so λ increases. From Figure 2A one can see the muon relaxation in ZF where there is the typical increase in λ_{ZF} that is due to the slowing down of electronic fluctuations. At low temperatures the electronic fluctuation rate flattens out and one sees a plateau in λ_{ZF}. If the relaxation rate enters a plateau region, this can mean that there are persistent dynamics, however in this case it could also be representative of the rigid lattice from quasi-static electronic moments. The associated relaxing asymmetry shows a gradual decrease as the sample goes through the transition. This is typical of a magnetic system entering an ordered state where the internal fields gradually grow and are large enough that they dephase the muon polarisation outside of the time scale of our measurement. This scenario leads to a missing fraction of asymmetry and in TEA(TCNQ)2 the magnetic transition results in a drop in asymmetry congruent with the onset of an ordered magnetic state, similar to what has been seen in both ferro- as well as antiferromagnets. Other spin-Peierls systems have shown no drop in the asymmetry as they are strongly dependent on singlet-triplet excitations but it is not regarded as a ferromagnetic (or antiferromagentic) ground state.

TF-μSR data were collected in an applied field of 50 G where raw data were best fit using the function:

$$G(t) = A_{TF}\cos(\omega t + \phi)\cdot\exp(-\lambda_{TF}t), \quad (3)$$

where the ω is the muon rotational frequency, ϕ is a phase offset and λ_{TF} is the muon relaxation in TF. λ_{TF} shows a strong temperature dependence and there is a prominent rise at around 110 K where the electronic fluctuation rate enters the experimental time window (see Figure 2B). There is then a peak at 70 K, which is where the fluctuation rate freezes out and the sample begins to enter a quasi-static state thus leading to a decrease in λ_{TF}. There is also a decrease in the relaxing asymmetry that is similar to the ZF experiment and points to the system entering a magnetically ordered phase where the internal fields are too strong and dephase the muon ensemble outside of the experimental time scale.

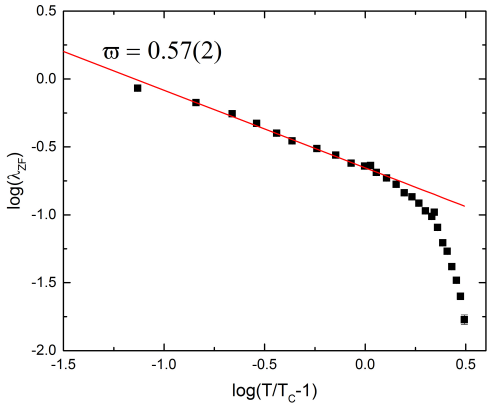

Fig. 3 log-log of plot of λ_{ZF} against reduced temperature where T_C to extract the dynamic exponent.

Interestingly, there is another upturn in the data at low temperatures that does not show an additional change in the asymmetry. Therefore it is not related to an emergent magnetic state. Instead, it could come from three different scenarios; the first being the onset of paramagnetic fluctuations on our time scale, the second being an additional exchange pathway becomes dominant and the system enters a glassy state or the upturn is due to defect spin causing the muon spin to relax. It is likely that the third scenario is the most plausible explanation as defect-defect interactions have been observed before in TCNQ based systems. How-

ever, it does provide insight into the low temperature behaviour of λ_{ZF}, where the flattening out at low temperatures is likely due to the onset of the electronic fluctuations of defect states.

In order to gain further information on the type of magnetic transition that the system undergoes, one can look at the critical behaviour of the fluctuation rate in ZF where one can use the equation

$$\lambda_{ZF} = Z\left(\frac{T}{T_C} - 1\right)^{-\varphi}, \quad (4)$$

where $T_C = 70$ K, Z is the pre-exponent and φ is the dynamic exponent. The log-log plot associated with Equation 4 can be seen in Figure 3 where if one takes the slope of this line in the linear region the fitted dynamic exponent is 0.57 ± 2. This matches well with the dynamic exponent expected for a 3D antiferromagnetic Ising system (0.596). This result implies that they system is entering a 3D magnetic state where the TCNQ interactions are antiferromagnetic and strongly anisotropic, perhaps aligning only parallel to the stacking axis of the TCNQ molecules. Since an electron is delocalised between two TCNQ molecules, and the electronic charge across the two molecules is not equal, this may result in a strongly anisotropic magnetic moment that can only point perpendicular to the flat plane of the TCNQ molecule. Extending this to a 3D system, the TCNQ dimer is strongly interacting and enters a 3D magnetic state where the internal fields at the muon site are large enough to cause dephasing outside of the experimental time scale.

4 Conclusion

An in-depth study of the magnetic transition in $TEA(TCNQ)_2$ has been performed using both magnetic susceptibility and muon spin spectroscopy measurements. The μSR results have provided insight into the nature of the magnetic transition where we were able to extract the dynamic exponent from the ZF data. This matched closely with that expected for a 3D antiferromagnetic Ising system which suggests that the system behaves like a 3D bulk material despite being quasi-1D in structure. It also highlights the complex nature of the delocalised electron across a TCNQ dimer where the electronic magnetic moment is strongly anisotropic and points long the stack and perpendicular to the flat plane of the TCNQ molecules.

Notes and references

1 S. Horiuchi and Y. Tokura. *Nat. Mater.*, 2008, **7**, 357

2 D. A. Bonnell. *Science*, 2013, **339**, 401

3 D.-W. Fu, H.-L. Cai, Y. Liu, Q. Ye, W. Zhang, Y. Zhang, X.-Y. Chen, G. Giovannetti, M. Capone, J. Li and R.-G. Xiong. *Science*, 2013, **339**, 425

4 A. A. Bokov and Z.-G. Ye. *J. Mater. Sci.*, 2006, **41**, 31

5 R. A. Cowley, S.N. Gvasaliya, S. G. Lushinikov, B. Roessli and G. M. Rotaru. *Adv. Phys.*, 2001, **60**, 229

6 F. Kagawa, T. Sato, K. Miyagawa, K. Kanoda, Y. Tokura, K. Koybayashi, R. Kumai and Y. Murakami. *Nat. Phys.*, 2013, **9**, 419

7 K. Miyagawa, A. Kawamoto, Y. Nakazawa and K. Kanoda. *Phys. Rev. Letts.*, 1995, **75**, 1174

8 P. Lunkenheimer, J. Muller, S. Krohns, F. Schrettle, A. Loidl, B. Hartman, R. Rommel, M. de Souza, C. Hotta, J. A. Schlueter and M. Lang. *Nat. Mat.*, 2012, **11**, 755

9 M. Poirier, M. de Lafontaine, C. Bourbonnais and J.-P. Pouget. *Phys. Rev. B.*, 2013, **88**, 245134

10 A. Filhol and M. Thomas. *Acta. Cryst.*, 1984, **B40**, 44

11 H. Koybayashi, Y. Ohashi, F. Marumo and Y. Saito. *Acta. Cryst.*, 1970, **B26**, 459

12 A. Brau, J.-P. Farges, A. Filhol and H. Grassi. *Phys. Stat. Sol. (b)*, 1983, **120**, 547

13 Organic Conductors: Fundamentals and Applications. J.-P. Farges. *CRC Press*, New York, 1994

14 J.P. Travers, F. Devreux and M. Nechtschein. *J. Phys. Coll.*, 1983, **44**, C3-1295

15 A. Filhol, C.M.E. Zeyen, P. Chenavas, J. Gaultier and P. Delhaes. *Acta Cryst. B*, 1980, **36**, 2719

16 S. Flandrois, J. Amiell, F. Carmona and P. Delhaes. *Sol. Stat. Comm.*, 1975, **17**, 287

17 J. S. Pedersen and K. Caneiro. *Rep. Prog. Phys.*, 1987, **50**, 995

18 J.-P. Farges. *J. Physique.*, 1985, **46**, 1249

19 L. R. Melby, R. J. Harder, W. R. Hertler, W. Mahler, R. E. Benson and W. E. Mochel. *J. Am. Chem. Soc.*, 1962, **84**, 3374

20 V. Zelezny, J. L. Musfeldt and D. B. Tanner. *Adv. Mater. Opt. Electr.*, 1996, **6**, 353

21 A. Brau and J.-P. Farges. *Phys. Stat. Sol. (b)*, 1974, **61**, 257

22 Frontiers of ferroelectricity: a special issue of the journal of Materials science. S. B.Lang and H. L. W. Chan. *Springer Science and Business Media*, 2007

23 J. P. Farges, A. Brau and F. Guttmann. *J. Phys. Chem. Solids*, 1972, **33**, 1723

24 J. P. Farges and A. Brau. *Phys. Stat. Sol. (b)*, 1974, **61** 669

25 W. Hu, Y. Liu, R. L. Withers, T. J. Frankcombe, L. Norén, A. Snashall, M. Kitchin, P. Smith, B. Gong, H. Chen, J. Schiemer, F. Brink and J. Wong-Leung. *Nat. Mater.*, 2013, **12**, 821

26 K. B. Lyons, P. A. Fleury and D. Rytz. *Phys. Rev. Letts.*, 1986, **57**, 2207

27 J.-P. Farges. *J. Phys.*, 1985, **46**, 465

28 Spin Glasses: An Experimental Introduction. J. A. Mydosh. *Taylor and Francis*, 1993

29 B. W. Lovett, S. J. Blundell, F. L. Pratt, Th. Jestadt, W. Hayes, S. Tagaki and M. Kurmoo. *Phys. Rev. B.*, 2000, **61**, 12241

30 J. Wu and C. Leighton. *Phys. Rev. B.*, 2003, **67**, 174408

31 F. Nad and P. Monceau. *J. Phys. Soc. Jpn.*, 2006, **75**, 051005

Conflicts of interest

There are no conflicts to declare.